JOURNAL OF MATERIALS SCIENCE 31 (1996) 3995–4005

The synthesis, characterization and sintering of sol–gel derived cordierite ceramics for electronic applications

D. PAL, A. K. CHAKRABORTY, SUCHITRA SEN
Central Glass & Ceramic Research Institute, Calcutta 700 032, India
S. K. SEN
Indian Association for the Cultivation of Science, Calcutta 700 032, India

Cordierite ceramics were synthesized by sol–gel processing using alkoxides and acetate with an aim to use the material as substrate and packaging material. Preparation conditions were optimized by varying the amount and pH of water added and the amount of acetic acid as chelating agent. The powders were characterized by different analytical techniques such as thermogravimetric analysis, differential thermal analysis, surface area by BET, X-ray diffraction, transmission and scanning electron microscopies and infrared spectroscopy. The best product was obtained using 19.6 mol water and 0.34 mol acetic acid with respect to silicon ethoxide. The pH of the water added did not make any significant difference. Sintered materials were characterized by measuring different physical properties such as density, electrical and dielectric properties, thermal expansion, microstructure and composition. Well-sintered bodies could be achieved at 1000 °C in air with a soaking time of 2 h having a density of ~ 99% theoretical, electrical resistivity of $\sim 10^{14}\ \Omega$cm, dielectric constant of 5, dielectric loss ~0.008 and thermal expansion coefficient of $28.5 \times 10^{-7}\,°C^{-1}$, 25–200 °C. X-ray diffraction studies show the phase evolution in these materials is predominantly μ-cordierite (hexagonal high cordierite) and some β-quartz. SEM reveals a uniformly dense microstructure with crystals of granular habit. X-ray photoelectron spectroscopy indicates that the surface composition of the sintered material is slightly enriched with aluminium and deficient in silicon.

1. Introduction

There are many important applications of ceramics and glass-ceramics in microelectronics, such as substrates in hybrid circuits and as packaging material in electronic packaging. The material which is almost exclusively used now-a-days for these purposes is alumina, because of its high electrical resistance, good thermal conductivity and high mechanical strength. But it also has several undesirable properties. The dielectric constant of alumina is quite high (~9) causing significant signal propagation delay in the device. Secondly, the thermal expansion coefficient of alumina is quite large ($52–74 \times 10^{-7}\,°C^{-1}$, 20–125 °C) which introduces stresses at the chip package interface. Finally, the sintering temperature of alumina is very high, ~1600 °C which restricts the choice of the metal for interconnections. The metals commonly used in alumina are tungsten, molybdenum and platinum [1]. A promising material, alternative to alumina, is based on cordierite composition ($2MgO \cdot 2Al_2O_3 \cdot 5SiO_2$) because of the low dielectric constant (5) and low thermal expansion coefficient matching silicon ($25–32 \times 10^{-7}\,°C^{-1}$, 20–125 °C). So, they are quite attractive to the electronics industry especially for high-frequency circuits.

Some investigations have already been done on these systems with different nucleating agents using the conventional glass-ceramics method to explore the potentiality of these materials in microelectronics [2, 3].

The conventional routes to prepare cordierite ceramics are (i) sintering from oxide powders and (ii) the glass-ceramics method. In the first method, stoichiometric cordierite is notoriously difficult to sinter without any sintering aid, because the temperature range available for sintering is very narrow and lies close to its incongruent melting temperature [4]. On the other hand, sintering aids degrade the desired dielectric properties. In the glass-ceramics method, the articles are made as monolithic glass wares and then a process of heat treatment converts the glass wares into glass-ceramics. During this heat-treatment process, large volume changes accompanying different stages of crystallization led to cracks in the articles. All these difficulties can be overcome by adopting a non-conventional method following the sol–gel route

0022–2461

TABLE I Characteristics of cordierite gels with experimental parameters

	Sample nomenclature	Amount of chelating agent(mol.ratio) (w.r.t. TEOS)	Molar ratio of water to TEOS	pH of water	gelation time (h)
1.	3/7	0.56	19.6	7	3
2.	3/2	0.56	19.6	2	3
3.	5/7	0.34	6.6	7	48
4.	5/2	0.34	6.6	2	48
5.	7/7	0.34	19.6	7	1
6.	7/2	0.34	19.6	2	1

which is based on low-temperature chemistry [5]. This method is notably recognized as a novel technique which offers control over homogeneity, stoichiometry as well as physical characteristics such as particle size, size distribution and morphology. Because of the finer particle size, the desiccated gels have higher free surface energy and as a result a significant reduction in sintering and densification temperature ($\sim 1000\,^{\circ}C$) occurs without any sintering aid. One can then use a more conducting metal, like copper, for interconnections which also possesses a lower melting temperature, high cohesive strength, good conductivity and good solderability. So the relevance of this work to the packaging industry is to synthesize a material sinterable at $\sim 1000\,^{\circ}C$ so that copper metallization can be used.

In this paper, the synthesis, characterization and sintering of pure cordierite ceramics prepared by sol–gel processing are described. Synthesis was carried out by optimising a few main preparation parameters.

The characterization was performed using different analytical tools and techniques such as surface area measurement by BET, differential thermal analysis (DTA), thermogravimetric analysis (TGA), infrared spectroscopy (IR) and X-ray analysis by diffraction measurement (XRD). Scanning electron microscopy (SEM) and transmission electron microscopy (TEM) have also been used to study the microscopic behaviour of the gels and sintered materials. Sintering of some of the well-characterized powders was carried out, their physical properties were measured and chemical composition was determined using X-ray photoelectron spectroscopy (XPS).

2. Experimental procedure

2.1. Synthesis of the powder

Several series of gel powders having the cordierite composition ($2MgO \cdot 2Al_2O_3 \cdot 5SiO_2$) were prepared from alkoxide precursors, silicon ethoxide ($Si(OC_2H_5)_4$(TEOS), aluminium secondary butoxide $Al(OC_4H_9)_3$ (AlOBt) and magnesium acetate tetrahydrate $Mg(OOCCH_3)_2 4H_2O$(MgAc). The solvent used was cellosolve, i.e. 2-methoxy ethanol ($C_3H_8O_2$) which was found to be very useful by us in other systems also [6]. A chelating agent (glacial acetic acid) was used to control the hydrolysis rate of AlOBt which has a very fast hydrolysis rate. A similar procedure has also been followed earlier by others in the TiO_2 system [7]. The role of the acetate ion is quite important in the mechanism of gelation. Because the preparation parameters are very important in gelation kinetics, gels were prepared in different ways. The parameters which were varied during preparation were (1) amount of chelating agent, (2) amount of water, (3) pH of water.

The molar ratios of acetic acid to TEOS used were 0.56 and 0.34. Because hydrolysis can also be controlled by varying the concentration of water [8], samples were made with two different molar ratios of water to TEOS (19.6 and 6.6). The pH of the water added was also varied (7 and 2). During gelation, the syneresis is sometimes observed. This effect is especially important where the duration of gelation is short. Shrinkage of about 50% is exhibited by this process. In Table I, a list of samples studied and their preparation parameters are shown.

The gels thus formed were allowed to dry at room temperature and finally dried at $130\,^{\circ}C$ in an air oven. These samples were then heated at $700\,^{\circ}C$ in oxygen for calcination at several steps in a furnace at a rate of $1\,^{\circ}C\,min^{-1}$ to obtain the amorphous powder.

2.2. Analysis of powder

The analysis of the powder was performed using the following analytical techniques.

DTA analysis was carried out in air up to $1200\,^{\circ}C$ at a heating rate of $10\,^{\circ}C\,min^{-1}$ using a NetZSCH 404 analyser (Germany). The crystalline phases and the resultant textures were determined using a Philips Geiger counter X-ray diffractometer model PW 1730 with nickel-filtered CuK_{α} radiation.

The microstructure of these powders was investigated in a Cambridge Steroscan S250 SEM and Jeol 200 kV TEM.

Thermogravimetric analysis was performed using the TGA apparatus at a rate of $1\,^{\circ}C\,min^{-1}$ up to $1000\,^{\circ}C$. The TGA curve was analysed to find the main peaks corresponding to main weight losses, and the soaking temperatures were selected accordingly. The surface areas of as-prepared and calcined powders were measured by the single-point BET method by nitrogen adsorption using an instrument of Carlo Erba Strmentazione (Italy). IR vibrational spectroscopy was performed with a Perkin–Elmer Fourier Transform IR spectrometer model 1750 in the wave number range 400–4000 cm^{-1}.

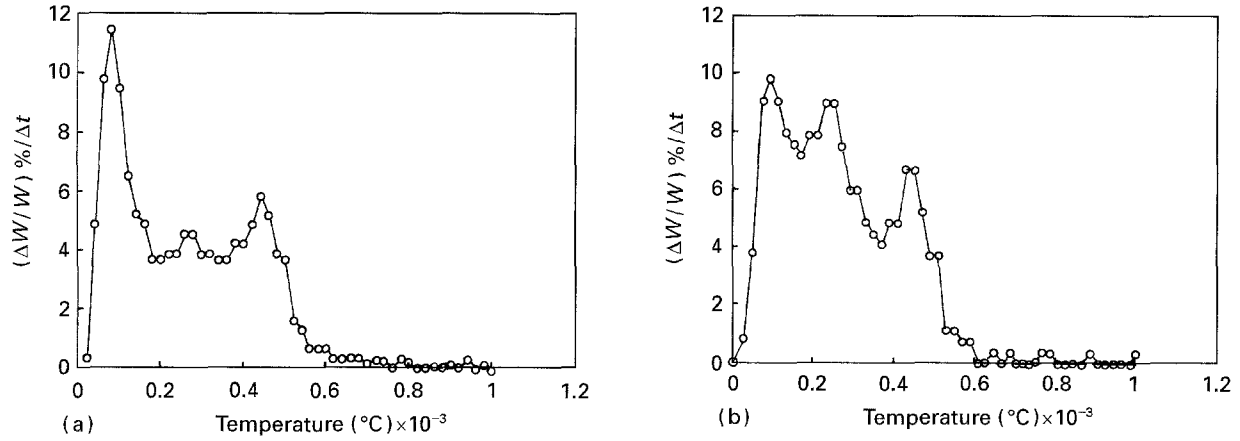

Figure 1 Differential TGA curve of cordierite gels prepared (a) without and (b) with acetic acid.

TABLE II Relative weight loss of gels with and without acetic acid

Type of gel	Temp. range (°C)	$\Delta W/W \times 10^3$	Colour of sample at 1000 °C
Gel without acetic acid	100–250	9.9	White
	250–450	12.8	
Gel with acetic acid	100–250	22.5	Dark grey
	250–450	16.9	

2.3. Sintering and subsequent characterization

For carrying out sintering work, the calcined powders were pelletized in a uniaxial press with a force of 1 ton to obtain a green compact of diameter 1.27 cm and thickness ~ 0.5–0.6 cm. The green density was measured as 40% of the theoretical density. It was sintered in an electric furnace at 1000 °C in air for 2 h. The sintered pellets thus obtained were then studied for different physical properties such as density, porosity, linear shrinkage, d.c. electrical resistivity, dielectric constant and loss, thermal expansion coefficient, microstructure and composition.

The d.c. electrical resistivity of sintered tablets was measured using a d.c. electrometer (ECIL make). The samples were kept in vacuum ($\sim 1 \times 10^{-3}$ torr; 1 torr = 133.322 Pa) on a teflon holder and the conventional three-probe method using a guard ring was applied to measure the resistivity. The dielectric properties, i.e. constant and loss, were measured at 1 MHz by the resonance method using a Boonton Q meter type 260 AP from Boonton Radio Corporation, USA. The thermal expansion of the sintered tablet was measured using a dummy standard sample of an aluminium rod of known thermal expansion in a dilatometer model 804, Bahr, Germany.

Microstructure of the sintered pellets was investigated in detail by SEM and TEM. For these purposes, the samples were polished to optical finish by diamond paste of grade 0.5 μm particle size, ultrasonically cleaned in isopropyl alcohol, then etched in 2%, 5%, or 10% HF, as required, for different lengths of time to reveal the microstructure clearly.

XPS was used to probe into the resultant chemical composition of the sintered pellets on an atomic scale from the surface layers of ~ 5–10 nm. The material was cleaned for sufficient time (~ 15 min) by an argon ion gun, model AgS2 using 8 kV and 100 μA current to remove the contaminant layers, and then the spectra were obtained in a VG-Microlab MK II instrument using MgK_α radiation (1253.6 eV).

3. Results and discussion

3.1. Thermogravimetric analysis

Thermogravimetric analysis of all the dried gel powders shows that three distinct temperature ranges of weight loss can be observed (Fig. 1a and b). The first peak appears around ~ 95 °C, which is due to the removal of physically adsorbed water. The second main peak appears in the temperature range 180–250 °C and corresponds to the oxidation of unreacted OR groups. The third peak appears around 400–450 °C and is probably associated with the removal of chemically bonded water [9]. The loss goes on even at higher temperatures upto 800 °C, as is evident from the appearance of many small peaks in this temperature range. These regions are quite distinct in the gel samples with acetic acid (Fig. 1b). The relative weight losses, $\Delta W/W$, of the gel powders are given in Table II and have been compared with gels prepared without acetic acid.

It is clear from these results that samples with acetic acid undergo a greater weight loss on heating compared to those without acetic aid. The colour of the sample after heat treatment at 1000 °C suggests that the pore size is much finer in the sample with acetic acid [9].

TABLE III Surface area of cordierite gels treated under different conditions

As-prepared			Calcined			
Sample	pH	Surface area ($m^2 g m^{-1}$)	Sample	pH	Calcination time at 700 °C (h)	Surface area ($m^2 g m^{-1}$)
3/2	2	402	7/2	2	1	256
3/7	7	440	7/2	2	16	166
5/2	2	303	7/7	7	1	255
5/7	7	358	7/7	7	24	42
7/7	7	344	5/7	7	1	~1
7/2	2	358				

The TGA results are very important in defining the calcination temperatures of the sample. The heat-treatment schedule for calcination, as mentioned in Section 2, was fixed following this curve. The temperature, 440 °C, is most important because at this temperature, burning of unreacted OR groups occurs. Hence during calcination the samples are kept for the maximum duration at this temperature.

3.2. Surface area analysis

The surface area of the powder was measured by the nitrogen adsorption method (BET) both in the as-prepared (oven dried) and calcined state. Table III shows at a glance the surface area values of these powders.

The materials prepared in the series of 3, 5 and 7 have reasonably good surface area in the as-prepared state, but after calcination at 700 °C, the surface area of series 5 of powder drastically falls down, whereas the series 7 powders retain a reasonably good surface area, even after calcination. Calcination at higher temperature, like ~ 800 °C, was not followed due to considerable agglomeration, as discussed later. The product after calcination is completely white. The reason for the very low value of surface area of series 5 powders may be due to the presence of carbon which is formed from unreacted OR groups. The probability is high because this powder was prepared by only 6.6 mol water which is insufficient for complete hydrolysis of the OR groups present in the gel material.

3.3. DTA

Phase transformations of the gel powder were studied using a differential thermal analyser. Fig. 2a–d shows some representative DTA curves of different series of cordierite powder. Cordierite gels, calcined for 16 h at 700 °C, 200–300 mesh size fractions, and a heating rate of 10 °C min^{-1} were used for differential thermal analysis. The traces for series 3 and 7 have similar features (Fig. 2a–c). Crystallization began between 929 and 934 °C and the crystallization rate reached maximum value in the range 966–974 °C. The second peak, which is not well resolved, and the third peak, occurred between 997 and 1002 °C and 1062 and 1086 °C, respectively. Identification of the phases is confirmed by XRD patterns of samples collected from the

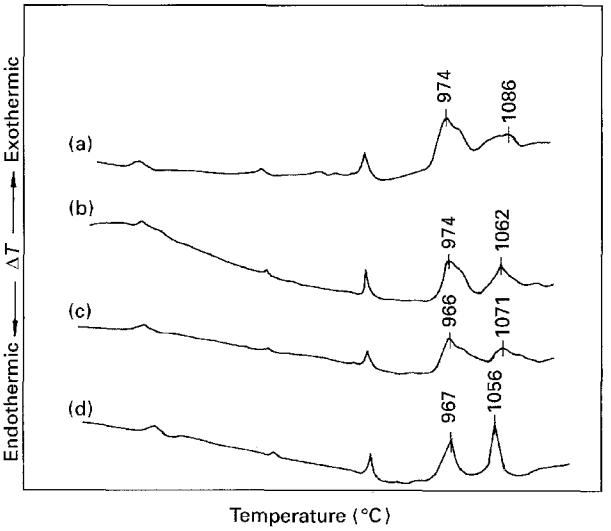

Figure 2 DTA curves of dried cordierite gels (a) 7/7, (b) 7/2, (c) 3/2, and (d) 5/2, up to 1200 °C.

exothermic peak temperatures. The first maximum corresponds to the formation of a metastable phase, i.e. stuffed β-quartz [10, 11]. The second peak, not well separated from first peak, is due to a trace amount of spinel. The third exothermic peak is attributed to the phase transformation of stuffed β-quartz to μ-cordierite (hexagonal high cordierite). For calcined cordierite powder of 5/2, no peak was observed for spinel. In this case, two exothermic peaks centred at about 967 and 1056 °C were identified by XRD as crystallization exotherms from amorphous to stuffed β-quartz and from stuffed β-quartz to hexagonal μ-cordierite, respectively. This observation is quite different from our earlier one on cordierite powder where we tried to optimize the dilution of the sol without any addition of water and acetic acid [11]. In the present work the initiation of crystallization is elevated by about 42–49 °C by adding water, whereas the conversion temperature of β-quartz to hexagonal μ-cordierite is aggravated at much lower temperature by about 100 °C. Thus the effect of the addition of water is advantageous in this case but the effect of adding acetic acid is not convincing.

3.4. XRD studies

X-ray diffraction studies reveal some important information regarding phase evolution and texture of

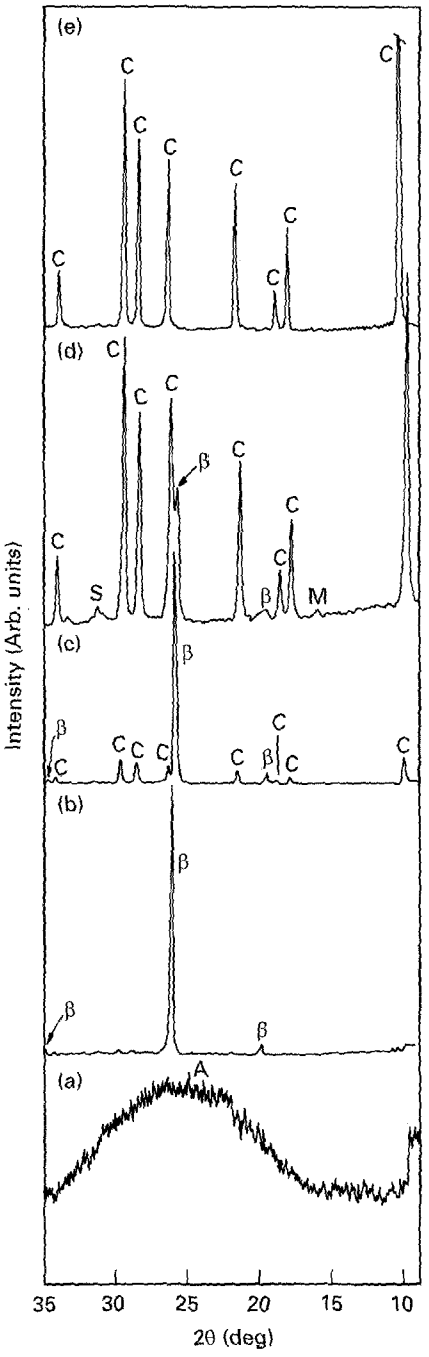

Figure 3 XRD patterns of dried series-7 cordierite gel (a) calcined at 700 °C, (b) 900 °C for 5 h, (c) 1000 °C for 1/2 h, (d) 1000 °C for 24 h, and (e) 1200 °C for 2 h. A, amorphous, β, stuffed β-quartz; S, spinel; M, mullite; C, hexagonal μ-cordierite.

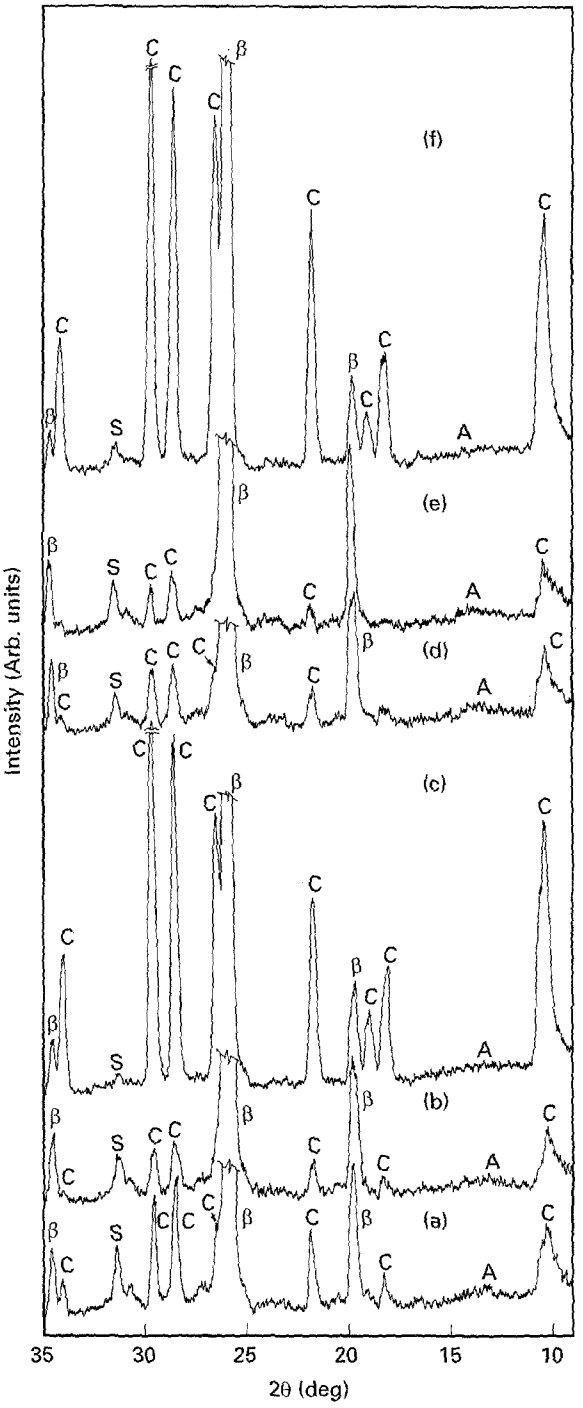

Figure 4 XRD patterns of different cordierite gels heat treated at 1000 °C for 1 h. (a) 3/2, (b) 3/7, (c) 5/2, (d) 5/7, (e) 7/7, and (f) 7/2. A, amorphous; β, stuffed β-quartz; S, spinel, C, hexagonal μ-cordierite.

the specimens, as depicted in Figs 3 and 4. Fig. 3 shows the progressive phase changes of a series 7 sample from amorphous to the crystalline state with increasing heat-treatment temperature. Fig. 4 shows the XRD patterns of different series of samples at 1000 °C. The difference in texture is apparent from Fig. 4. The matrix is amorphous at 700 °C. When the samples were heat treated at 900 °C for 5 h, stuffed β-quartz appeared as the main phase, whereas heat treatment at 1000 °C for different periods of time produces β-quartz, μ-cordierite and a trace of spinel (Fig. 3). Whether β-quartz or μ-cordierite appears as the major phase depends entirely on the total time of soaking at this temperature. For example, at 1000 °C, soaking for 1/2 h yields β-quartz as the major phase in all the sample series like 7, 3 and 5 (Fig. 3c). Increasing the soaking time to 1 h results in an equally strong presence of β-quartz and μ-cordierite. Soaking for 24 h results in the formation of μ-cordierite as the dominant phase. However, at this stage, the texture of the samples was found to be different in series 3 compared to series 7 and 5. In series 7 samples, a random texture was developed with (1 0 0) being the most intense plane, as reported in ASTM, whereas in series 3 samples, a different texture with (1 1 2) preferred orientation was observed. A general observation that can be made from these studies is that at 1000 °C the formation of μ-cordierite is greater with pH 2 samples. When heat treated at 1200 °C, in all the samples, the μ cordierite was developed as the single phase. This is

TABLE IV Lattice parameter values of μ-cordierite developed under different heat-treatment conditions

950 °C, 5 h		1000 °C, 2 h		1200 °C, 2 h	
a (nm)	*c* (nm)	*a* (nm)	*c* (nm)	*a* (nm)	*c* (nm)
0.9459	0.9234	0.9747	0.9330	0.9765	0.9330

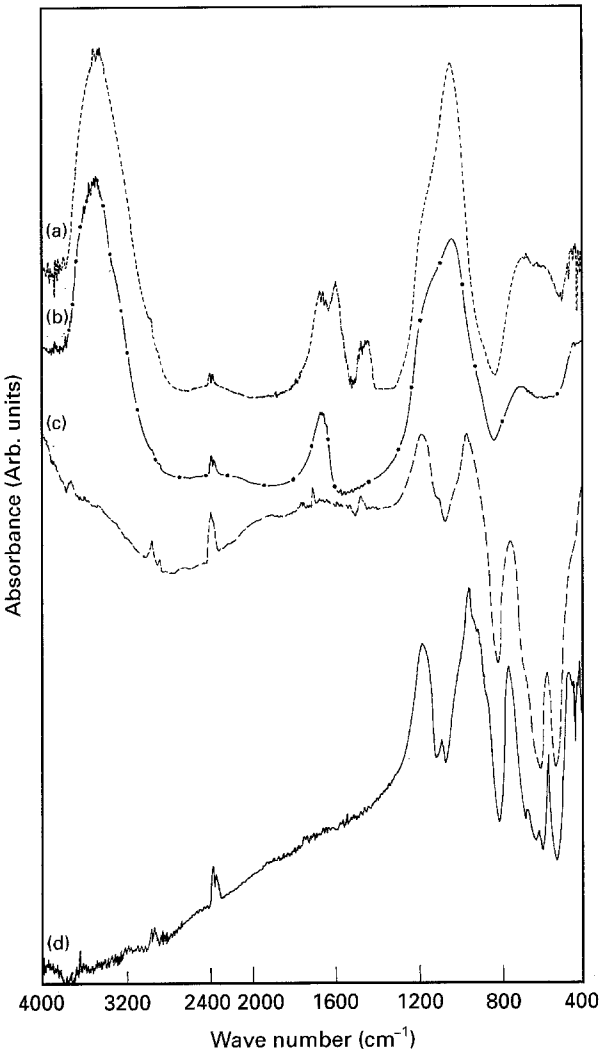

Figure 5 FT–IR spectra of KBr pressed pellet of series 7 cordierite gel heat treated at (a) 130 °C, (b) 700 °C, (c) 1000 °C, (d) 1200 °C.

in accordance with the observation of Gensse and Chowdhury [10]. The lattice parameters of phases developed at different temperatures were calculated from peak positions and are shown in Table IV.

3.5. IR studies

It is a common practice to follow the ordering processes in the study of polymorphic transitions of cordierite and other systems using infrared techniques. Previously, such investigations have been used to identify the devitrification products of cordierite [10], magnesium-cordierite glass [12], β-eucryptite [13] and mullite [14] combining X-ray diffraction studies with IR investigation. We have also performed IR studies at different stages of the material preparation

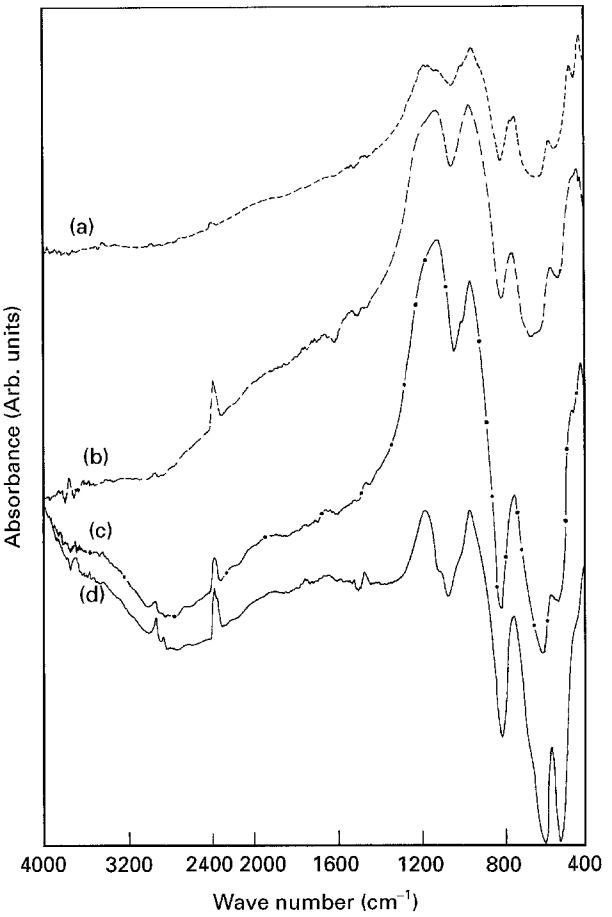

Figure 6 FT–IR spectra of KBr pressed pellet of different cordierite gels heat treated at 1000 °C; (a) 3/7, (b) 5/7, (c) 7/2, (d) 7/7.

to understand the structural changes in these materials.

The spectra of a sample of series 7 at different stages of its thermal history have been displayed in Fig. 5. Similarly, Fig. 6 shows the spectra of some samples having different preparation parameters soaked at 1000 °C for 1 h. The measured wave numbers of all the absorption bands are listed in Tables V and VI, respectively.

Generally, the IR spectra of SiO_2 polymorphs constituted by tetrahedrally coordinated silicon atoms are characterized by three groups of bands: (i) strong bands whose maximum is detected in the 1110–1090 cm^{-1} region, (ii) medium intensity band in the range of 820–650 cm^{-1}, and (iii) one or more strong band in the region 500–400 cm^{-1}. The first set of bands corresponds to asymmetric Si–O–Si stretching modes, the second bands to the symmetric mode and the third ones can be assigned to deformation modes.

The spectrum recorded on a xerogel dried at 130 °C (Fig. 5a) for 24 h shows two broad bands at 422 and 679 cm^{-1} and one peak around 1024 cm^{-1}. The two peaks appearing around 1459 and 1579 cm^{-1} suggest the presence of chelating acetate groups [7]. The separation of these two bands on a frequency scale is ~120 cm^{-1}. This is evidence that CH_3COO acts as a bidentate ligand. The band at 1656 cm^{-1} probably corresponds to OH stretching mode. All three of these peaks at higher wave number gradually disappear

TABLE V Position of absorption band maxima in the IR spectra of sample 7/7 at different heat-treatment temperatures

120 °C	700 °C	1000 °C	1200 °C
422 *b*	450	400	426
		465 *s*	457 *b*
		576	577 *m*
		670 *s*	625 *w*
			679 *w*
679 *b*	706 *b*	752	767 *s*
		958	954 *vs*
		1090 *s*	1091 *msh*
1024	1029	1173	1179 *s*
1459		1465 *w*	
1579			
1656	1655	1657 *wb*	

s, strong; *b*, broad; *w*, weak; vs, very strong; *m*, medium; *sh*, sharp.

TABLE VI Comparison of absorption band maxima of different samples heat treated at 1000 °C

3/7	5/7	7/7	7/2
429	442	400	427
474		465	470
572	566	576	566
741	747	752	742
941	947	958	947
1159	1110	1090	1154
	1173	1173	
1445	1460	1465	1450
1460			
	1645	1657	1650

with annealing, finally leaving no trace at 1200 °C. The first three peaks are slightly shifted towards higher wave numbers when annealed at 700 °C (Fig. 5b). If we study the IR spectra of series 3, 5, and 7 samples calcined at 700 °C, it is observed that all the samples are amorphous with broad bands, which is in agreement with the X-ray results.

If we look at the IR spectra of a series 7 sample annealed at 1200 °C (Fig. 5d), we can isolate three peaks, of which the two at 1091 and 1179 cm^{-1} correspond to Si–O–Si asymmetric stretching while that at 954 cm^{-1} has the character of symmetric stretching of AlO_4 tetrahedra. The strong band at 954 cm^{-1} should not be present in silica polymorphs. It may be due to the Si–O terminal bond, which is not expected in these types of material. So this has been assigned to the vibration of AlO_4 tetrahedra by Mazza *et al.* [13].

The bands at 679 and 767 cm^{-1} are due to the symmetric stretching mode of the Si–O–Si bond but their positions are not at lower frequencies than in the case of silicon polymorphs, as was earlier found by Mazza *et al.*

The broad band at 457 cm^{-1} can be assigned to the deformation mode, whereas that at 577 cm^{-1}, which is rather strong, has been assigned to the vibrations of MgO_4 stretching because it is not found in silica polymorphs. This is found to be at a slightly higher wave number side than that found by Mazza *et al.* (542 cm^{-1}), but it is closer to that (578 cm^{-1}) found by Langer and Schreyer [12].

From Fig. 6 and Table VI it is evident that at 1000 °C most of the bands of different samples are shifted down the wave number side; less so for the sample 7/7. So considering all these factors, it seems that the sample prepared under the conditions mentioned for series 7/7 achieved the required structure.

3.6. TEM and SEM observations

The TEM microstructure of the gel samples prepared under different conditions has been studied in order to determine whether the densification of the gel powders depends on the microstructure (Fig. 7a–c). In dried cordierite gel powder, samples of series 3 and 7, it is observed that irregular shaped features, which are just polymer clusters of low electron density contrast, appear in the transmission electron micrograph, with some high-contrast regions inside them. These high-contrast regions appear to be particulate, the size being in the range 4–8 nm. So the feature, as a whole, appears to be some kind of particulate nature in the case of series 7 and 3 (Fig. 7a). The low electron density region is probably the dried solvent region and the high electron density region is the material-rich region. Because our system is multicomponent, it is hard to say from the micrograph whether the material-rich region is homogeneous or rich in some particular oxide component. The pores are very fine, lying in the range 2–6 nm. All these observations seem to be topologically very similar to that observed in the base-catalysed silica system [15], although it is not known whether we can draw an analogy between microstructure of a multicomponent system of silica to that of a simple silicate system. In series 5 samples,

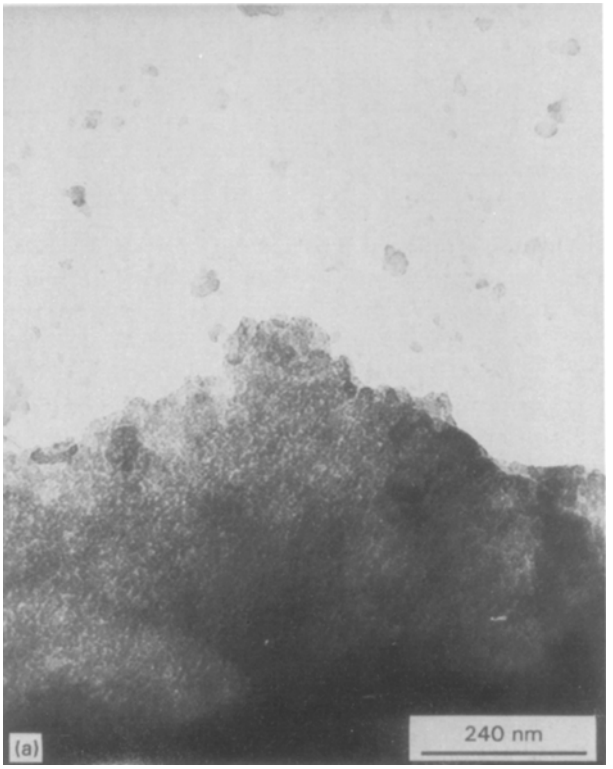

Figure 7 Transmission electron micrographs of cordierite gel; (a) 7/7, (b) 7/2, and (c) 5/2.

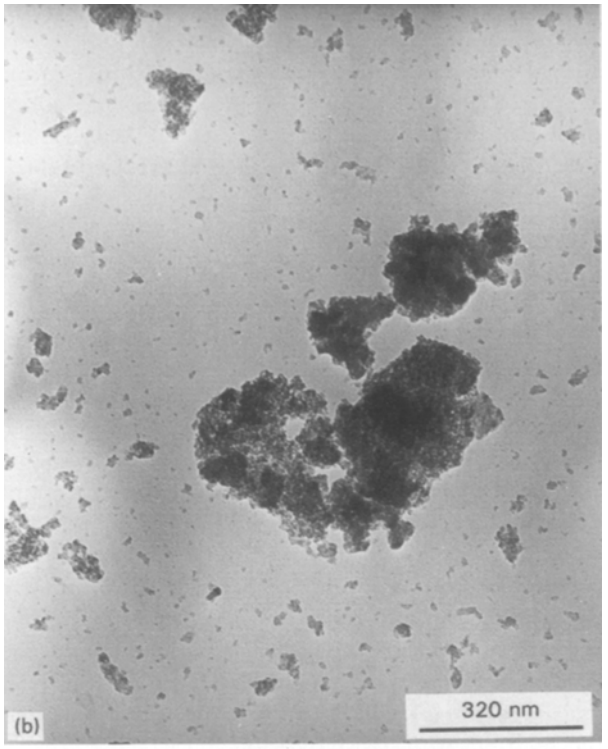

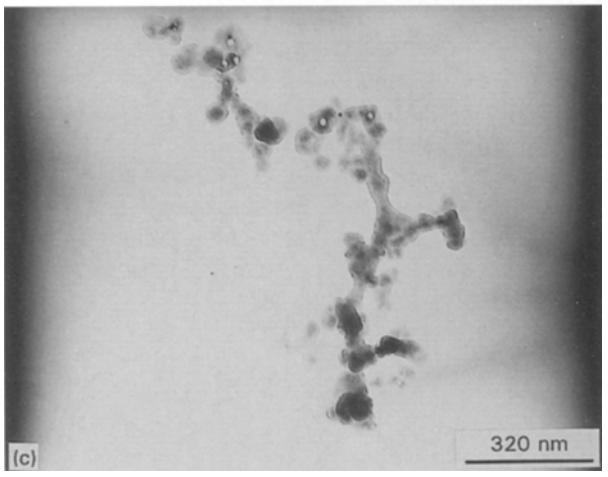

Figure 7 Continued.

the feature is different. The micrograph (Fig. 7c) shows that the gel possesses a chain-like structure which again consists of high- and low-contrast regions. It is clear from the micrograph that the high-contrast region consists of particles of size ~10–20 nm. The composition of the low-contrast region is not clear. This observation is similar to that observed by Brinker and Scherer [16]. Thus, from the TEM observations, we can conclude that more or less the same features are observed in all the gel samples except in series 5. There are elongated particles whose dimensions are similar. In samples prepared with pH2 water, the particulate nature is more distinct (Fig. 7b).

SEM investigation was performed on calcined cordierite powder for optimization of the calcination conditions. Fig. 8a and b show some representative cases. Fig. 8a, calcined at 700 °C shows well-dispersed particles of average size ~350 nm. It shows a much less degree of agglomeration when compared to that calcined at 800 °C (Fig. 8b). Hence, powders calcined at 700 °C were chosen for sintering work.

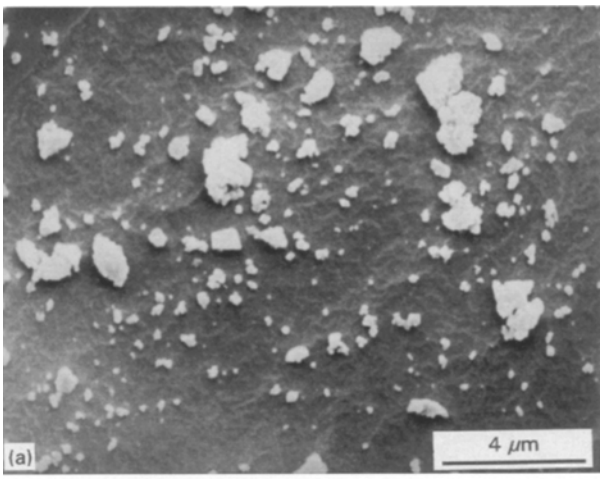

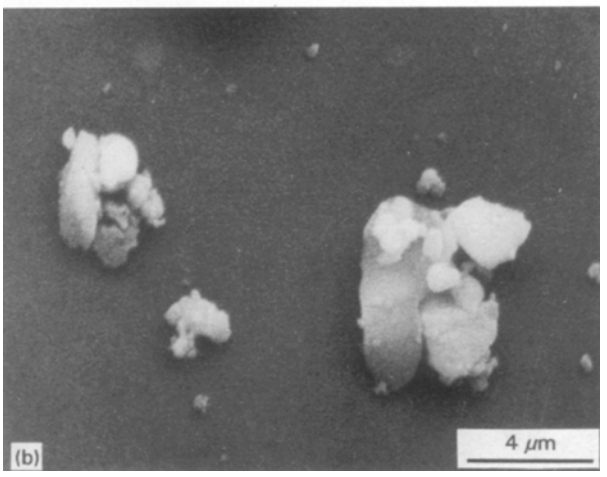

Figure 8 Scanning electron micrographs of series 7 cordierite gel; (a) 700 °C and (b) 800 °C.

3.7. Sintering and subsequent characterization

If the densification of a pure and homogeneous cordierite powder compact occurs below the crystallization temperature, it would be possible to obtain pure and dense cordierite ceramics with relatively high flexural strength and a low thermal expansion coefficient. So, the sintering of the calcined powders was carried out next.

The data of as-prepared powder as well as of calcined powder show that the powders of series 3 and 7 show good characteristics such as high surface area, large weight loss, and the desired phase evolution, from the X-ray, and DTA results. This led us to work with these two series of powders for sintering, namely 3/2, 3/7, 7/2, and 7/7 whereas 5/2 and 5/7 powders were also tried for comparison.

It was observed that both series 3 and 7 powders could be well sintered at this temperature, but series 5 could not be sintered at all where there was a problem of bloating and foaming. This was also observed earlier by other workers in the pure silica system [17]. Because series 3 powders showed characteristics quite

TABLE VII Physical properties of sintered cordierite

Sample	Density ($g\,cm^{-3}$)	Linear shrinkage (%)	Water absorp. (%)	D.c. elec. resist. (Ω cm)	Dielec. const. at 1 MHz	Tan δ	Coeff. therm. exp. ($10^{7}\,°C^{-1}$)
7/7	2.496	32	0.5	$\sim 10^{14}$	4.80	0.0083	28.5 (25–200 °C)
7/2	2.49	29	–	$\sim 10^{14}$	5.15	0.0076	–

similar to series 7, the latter were ultimately chosen for sintering.

Sintering at 1000 °C was carried out on samples having a particle size in the range -200 to $+300$ mesh. Table VII lists some of the important physical properties measured in our laboratory.

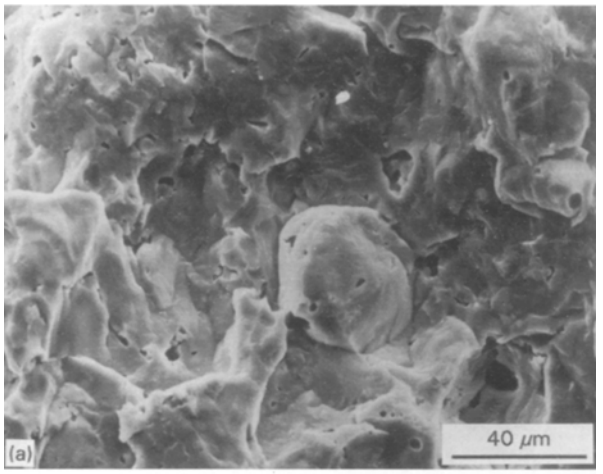

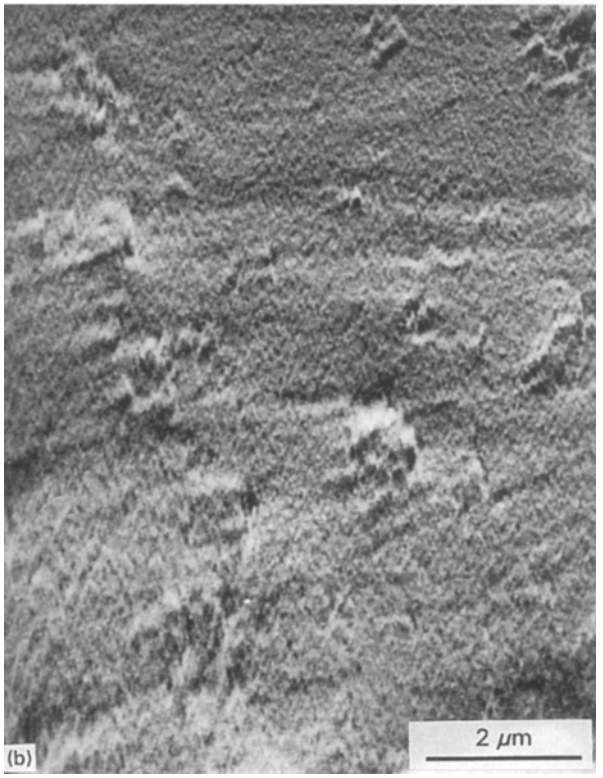

Figure 9 Scanning electron micrograph of sintered cordierite of series 7; (a) fractured surface, (b) polished surface: Y mod., (c) polished surface, and (d) polished surface. (c) Sintered 950 °C, 5 h; (a, b, d) sintered 1000 °C, 2 h.

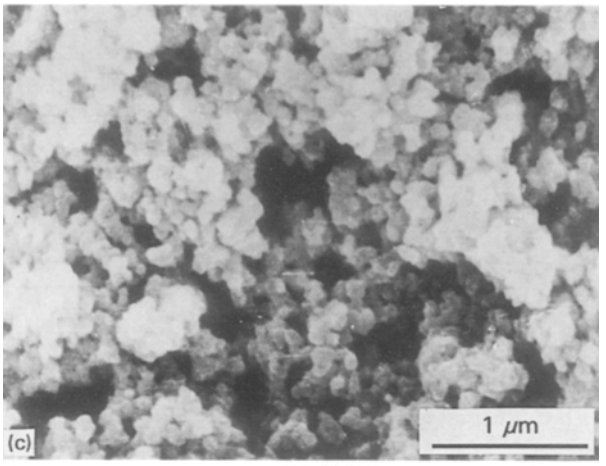

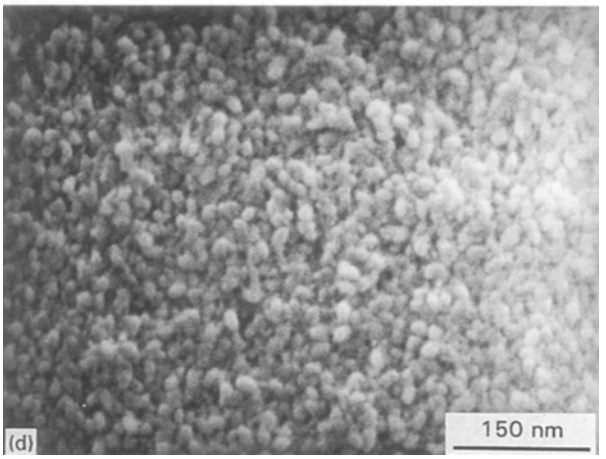

Figure 9 Continued.

3.7.1. Microstructure

The series of scanning electron micrographs (Fig. 9a–d) was taken both on freshly fractured and polished surfaces. Fig. 9a, taken on a fracture surface, shows the microstructure of a sintered cordierite pellet of series 7. A number of such micrographs were taken for calculating the porosity distribution by the 100 point grid method [18] and it was found that about 2%–3% porosity is developed in this material. Fig. 9b was taken in the Y-modulation mode and shows the topography of the surface of the sintered cordierite pellet much more clearly.

Fig. 9c and d were taken on polished surfaces etched in HF and sintered at different temperatures. Fig. 9c is from a sample sintered at 950 °C for 5 h and Fig. 9d is taken from a sample sintered at 1000 °C for 2 h. From the micrograph, it is clear that sintering at 1000 °C produced a much denser material than at

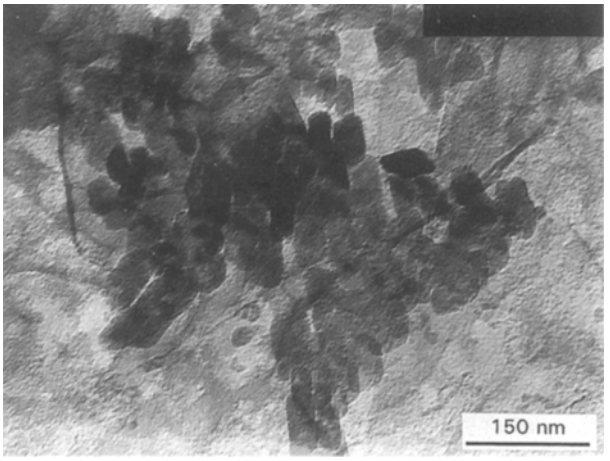

Figure 10 Transmission electron micrographs of a carbon replica of a polished surface of sintered cordierite.

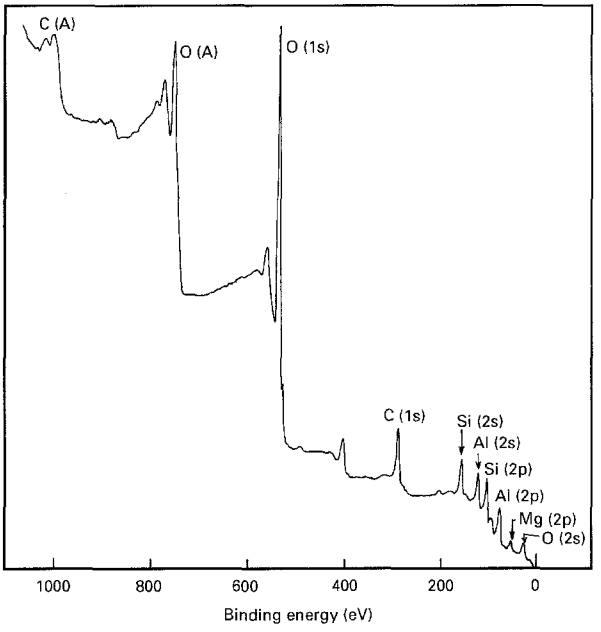

Figure 11 XPS survey scan of series 7 sintered cordierite in the binding energy range of 0–1100 eV.

950 °C. At 1000 °C the matrix is composed of crystals of granular habit and the grain size is of the order of 100 nm.

TEM was also performed on a sintered cordierite body by the two-stage carbon replica method. Fig. 10 shows such a case. It presents a representative bright-field image of the sintered body of a sample of series 7. It is evident that the habits of the crystals are well developed and the size ranges from 30–100 nm, which corresponds well to the SEM observation. The average thickness of the glassy phase surrounding the cordierite grains is about 10 nm, or even less.

3.7.2. XPS study

Fig. 11 shows the XPS spectra of a sintered sample of series 7 in the binding energy range of 0–1100 eV. The elemental identification shows the presence of all the major elements present in cordierite. Until now, there have only been a few reports on XPS data of the cordierite system [19, 20]. In Table VIII, we have reported the binding energy values of the strong lines of the elements and compared them with the values reported earlier. The charge compensation has been done using C 1s as an internal standard. It is evident from the table that there is close similarity between our results and those of Werckmann *et al.* [20]. The relative elemental concentration was performed with the peak area measurements of the major elements using tabulated sensitivity factors [21]. We obtained for the sintered sample, the atomic concentrations of 17% Al, 7% Mg, 15% Si and 61% O, which is close to the theoretical composition of 14% Al, 7% Mg, 17% Si and 62% O. Considering an error of $\pm 10\%$ in composition measurement by XPS, the values indicate the right stoichiometry of oxygen and magnesium, but a slight deficiency of silicon and an enrichment of aluminium.

TABLE VIII Photoelectron binding energy, E_b, values measured on sintered cordierite, and comparison with earlier measurements

Peaks	E_b (eV)		
	Present	Werckmann *et al.* [20]	Bortz and Ohuchi [19]
O 1s	531.9	532.0	–
Al 2p	74.8	74.8	75.4
Mg 2s	89.9	–	–
Mg 2p	51.3	51.1	51.7
Si 2p	102.6	102.0	103.8

4. Conclusion

We have successfully synthesized stoichiometric cordierite gel by a sol–gel process after optimizing the preparation conditions. The main parameters for optimization were the amount and pH of water and the amount of acetic acid as chelating agent. It was observed that the molar ratio of water played the most important role in the synthesis. Detailed characterization by different analytical techniques such as TGA, BET, XRD, TEM, SEM and IR, show that the gels prepared with 19.6 mol water and 0.34 mol acetic acid produced a powder which is sinterable at $\sim 1000\,^{\circ}C$ in 2 h in air. The sintered product has a density of ~98%–99% theoretical, an electrical resistivity of $\sim 10^{14}\,\Omega$ cm, a dielectric constant of ~5, a dielectric loss of ~ 0.008, and a coefficient of thermal expansion of $\sim 28.5 \times 10^{-7}\,^{\circ}C^{-1}$, 25–200 °C. All these indicate the promise of these materials as potential candidates in electronic applications. XRD shows the presence of mainly μ-cordierite (hexagonal high cordierite) and β-quartz at 1000 °C developed during sintering, which could be transformed to μ-cordierite completely at 1200 °C. Microstructural investigation shows a dense material with well-developed crystals of ~100 nm in size. XPS study reveals that the surface composition of the material is close to the stoichiometric cordierite composition of 2:2:5, except for a slight depletion in silicon and enrichment in aluminium.

Acknowledgements

The authors are grateful to Dr B. K. Sarkar, Director, C.G.C.R.I., for permission to publish this paper. They thank Sri Arup Ghosh, D. Chatterjee, S. Bose and Dr A. K. Chakraborty for their help in BET, XRD, thermal expansion and dielectric property measurements, and Sri R. K. Mondal, H. Majumdar, Sm. S. Roy, A. Laskar and Dr S. K. Pradhan for their co-operation during the course of the work. They are grateful to Dr R. Banerjee, I.A.C.S, Calcutta, for IR investigation, and to R.S.I.C., Bose Institute and Biophysics division, S.I.N.P. of Calcutta, for TEM facilities.

References

1. B. SCHWARTZ, *J. Phys. Chem Solids.* **45** (1984) 1051.
2. G. PARTRIDGE, C. A. ELYARD and H. D. KEATMAN, *Glass Technol.* **30** (1989) 215.
3. D. R. BRIDGE, D. HOLLAND and P. W. McMILLIAN, *ibid.* **26** (1985) 286.
4. R. MORRELL, *Proc. Br. Ceram. Soc.* **28** (1979) 53.
5. J. ZARZYCKI, *J. Non-cryst. Solids* **46** (1982) 105.
6. P. KUNDU, D. PAL and SUCHITRA SEN, *J. Mater. Sci.* **23** (1988) 1539.
7. S. DOEUFF, M. HENRY, C. SANCHEZ and J. LIVAGE, *J. Non-Cryst. Solids* **89** (1987) 206.
8. H. SUZUKI, O. KAZUHIDE and S. HAJIME, *Yogyo-Kyokai-Shi* **95** (2) (1987) 32.
9. SUCHITRA SEN and J. ZARZYCKI, 1990.
10. C. GENSSE and U. CHOWDHURY, *Mater. Res. Soc. Symp. Proc.* **73** (1986) 693.
11. D. PAL, S. SEN, A. K. CHAUDHURI and S. THIAGARAJAN, *Ind. J Phys.* **63A** (1989) 472.
12. K. LANGER and W. SCHREYER, *Am. Mineral.* **54** (1969) 1442.
13. D. MAZZA, M. LUCCO-BORLERA, G. BUSCA and A. DELMASTRO, *J. Eur. Ceram. Soc.* **11** (1993) 299.
14. SUCHITRA SEN and S. THIAGARAJAN, *Ceram. Int.* **14** (1988) 77.
15. J. K. BAILEY, T. NAGASE, S. M. BROBERG and M. L. MECARTNEY, *J. Non-Cryst. Solids* **109** (1989) 198.
16. C. J. BRINKER and G. W. SCHERER, *ibid.* **70** (1985) 301.
17. N. DELA ROSA-FOX, L. ESQUIVIAS and J. ZARZYCKI, *ibid.* **89** (1987) 206.
18. A. PHILLIPS, V. KERLINS, R.A. RAWE and B. V. WHITESON, "Electron Fractography Handbook: Metals and Ceramics Information" edited by Dept. of Defence Information Analysis Center (Battelle, Ohio, 1976) p. 55.
19. M. BORTZ and F. S. OHUCHI, *J. Appl. Phys.* **64** (1988) 2054.
20. J. WERCKMANN, P. HUMBERT, C. ESNOUF, J. C. BROUDIC and S. VILMINOT, *J. Mater. Sci.* **28** (1993) 5229.
21. P. M. A. SHERWOOD, in "Practical surface analysis by Auger and X-ray photoelectron spectroscopy" edited by D. Briggs and M. P. Seah (Wiley, New York, 1983) p. 445.

Received 8 August
and accepted 21 December 1995